

# Electron Spin Resonance Studies of Order and Dynamics in a Nematic Liquid Crystal Containing a Dispersed Hydrophobic Aerosil

Alberto Arcioni,<sup>†</sup> Corrado Bacchiocchi,<sup>†</sup> Loris Grossi,<sup>‡</sup> Alessandro Nicolini,<sup>†</sup> and Claudio Zannoni<sup>\*,†</sup>

Dipartimento di Chimica Fisica e Inorganica, Università, Viale Risorgimento 4, I-40136 Bologna, Italy, and Dipartimento di Chimica Organica "A. Mangini", Università, Viale Risorgimento 4, I-40136 Bologna, Italy

Received: February 27, 2002; In Final Form: June 27, 2002

We have studied a system composed of a hydrophobic aerosil (R812) dispersed in the liquid crystal 4-*n*-octyl-4'-cyanobiphenyl (8CB) using the spin probe electron spin resonance (ESR) technique, and in particular, we have determined, for different aerosil concentrations, the temperature dependence of the orientational order parameter,  $\langle P_2 \rangle$ , and the rotational diffusion coefficient,  $D_{\perp}$ , of the probe 5-doxyl stearic acid in the ordered and isotropic phases of the system. We have found that increasing the silica concentration up to 10 wt % does not significantly change the transition temperatures of the system. The probe order parameter is instead depressed, and we found that the  $\beta$  exponent of an empirical Haller-type equation, used to fit its temperature dependence, changes roughly linearly with the aerosil concentration. The concentration effect on the probe dynamics is relatively small in the isotropic phase, where the  $D_{\perp}$  temperature dependence is well fitted for all of the systems with an Arrhenius-type equation. In the nematic phase, the dynamical behavior is more complex: we found that, while local probe motion is still rather fast even when the macroscopic behavior is gellike, the temperature dependence of  $D_{\perp}$  is still of Arrhenius-type up to 3 wt % aerosil concentration but it becomes of Vogel–Fulcher–Tammann-type for the 10 wt % R812 system.

## 1. Introduction

Liquid crystals<sup>1</sup> containing a suspension of pyrolytic silica particles (aerosils<sup>2</sup>) of nanometric size present fascinating fundamental<sup>3</sup> and applicative aspects.<sup>4</sup> From the fundamental point of view, the interest stems from the intricacies of the effect of a random perturbation on ordered phases, with the silica particles playing the role of the perturber. In particular, according to the "Imry–Ma argument", an arbitrarily low amount of static disorder should suppress long-range order (LRO) in a large enough continuous symmetry system in three dimensions.<sup>3,5</sup> The system also presents technological interest in view of scattering displays with memory.<sup>4</sup> In these displays, the nematic "filled" with a small concentration of aerosil (up to a few percent) strongly scatters light in its field-off state because of the large optical anisotropy of the macroscopically disordered nematic. Application of an electric field aligns the nematic domains yielding a transparent state, and for appropriate combinations of aerosil type and liquid crystal, this clear state remains even after removal of the field ("memory effect"). Notice that the small concentration of silica does not change the optical properties of the liquid crystal by itself; indeed no optical matching between liquid crystal and aerosil is needed. The display can be easily switched back to its scattering state in various ways, for example, thermally by application of a focused laser beam.<sup>6</sup>

Eidenschink and de Jeu explained the electrooptical behavior assuming the formation of a network of aerosil particles and

liquid crystal.<sup>7,8</sup> This process is more understandable in aerosils with dangling silanol groups in which hydrogen bonding can lead to diffusion-limited aggregation, if the silica density exceeds the gelation threshold ( $\sim 0.01$  g/cm<sup>3</sup> for a hydrophilic aerosil<sup>9</sup>). However, the effect is obtained both with hydrophilic (e.g., type 300) and hydrophobic (e.g., type R812) aerosils.

A number of these systems have been studied using macroscopic level techniques. Iannacchione et al.<sup>10</sup> performed a high-resolution calorimetric study of the nematic and smectic phase transitions as a function of the aerosil density for different dispersions of type 300 hydrophilic aerosil particles in 4-*n*-octyl-4'-cyanobiphenyl (8CB) liquid crystal. They found that, as the aerosil concentration is increased from  $\sim 0.02$  to  $\sim 0.4$  g/cm<sup>3</sup>, both the nematic–isotropic (N–I) and the smectic A–nematic (SmA–N) transitions exhibit shifts to lower temperatures. For silica densities below  $\sim 0.1$  g/cm<sup>3</sup>, sharp, second-order  $C_p$  peaks for the SmA–N transition and two closely spaced first-order peaks for the N–I transition are observed. At higher densities only a single, rounded peak is observed for both transitions with a decrease in the total enthalpy.

A decrease of the N–I and the SmA–N transition temperatures with increasing aerosil concentrations was also found by Marinelli and co-workers<sup>11,12</sup> who recently reported on high-resolution photopyroelectric measurements of homeotropically aligned hydrophilic aerosil dispersions in 8CB at a lower concentration range: from 0.005 to 0.04 g/cm<sup>3</sup>. Interestingly, their thermal conductivity data showed hysteresis for all of the mixtures, indicating that the elastic strain, due to the presence of the aerosil particles, is not completely annealed at the N–I transition if the sample is cooled from the I phase.

High-resolution ac calorimetric studies of 8CB containing a hydrophobic aerosil (R812) were performed by Zhou et al.<sup>13</sup> Only a small shift ( $< 1$  °C) was found for silica concentrations

\* To whom correspondence should be addressed. Fax: + 39 051 644 7012. E-mail: claudio.zannoni@cineca.it. URL: <http://www.fci.unibo.it/~bebo/z/>.

<sup>†</sup> Dipartimento di Chimica Fisica e Inorganica.

<sup>‡</sup> Dipartimento di Chimica Organica "A. Mangini".

up to 10% (0.1 g/cm<sup>3</sup>) in the N–I and the SmA–N transition temperatures. Differently from silica aerogels<sup>14</sup> of comparable density, the specific heat peak of the SmA–N transition remains sharp even if, with increasing silica concentration, it decreases in intensity and eventually disappears.

Even if at the moment less interesting for display applications, the smectic region is of particular interest for understanding the effect of random perturbations, because theory<sup>15</sup> predicts destruction of orientational as well as translational ordering in the presence of random disorder with the formation of glassy states.

Type R812 hydrophobic aerosil–liquid crystal suspensions have been studied experimentally using optical techniques, for example, scattering and transmission,<sup>3,4,16</sup> and using a more viscous, cholesteric liquid crystal by AFM.<sup>17</sup> R812 aerosil has also been used in erasable bistable displays.<sup>6,16</sup> In particular, for a dispersion of R812 aerosil in 4-*n*-pentyl-4'-cyanobiphenyl (5CB) liquid crystal, a maximum of the memory effect was found for an aerosil concentration between 8 and 12 wt %.<sup>16</sup> Interestingly enough, optical turbidity studies<sup>3</sup> show that the liquid crystal loses true long-range order upon addition of the aerosil and that the residual order is short range with respect to the optical wavelength and scales with the disordering silica particles concentration.

Molecular level studies of ordering are scarce, but disordering effects due to different concentrations of type 300 hydrophilic aerosil particles dispersed in 8CB have been recently studied using deuterium NMR.<sup>9</sup> The results were discussed within the assumption that the hydroxyl groups covering the aerosil particles form hydrogen bonds with the 8CB cyano group, producing a homeotropic anchoring at the silica surfaces and causing elastic strains that increase with increasing aerosil density. In low-concentration dispersions (less than 0.1 g/cm<sup>3</sup>), the orientational order was found to be essentially bulklike possibly corresponding to these elastic strains being partially annealed. The presence of the NMR magnetic field contributes to make the annealing more complete because of field-induced alignment of the 8CB molecules. The behavior of the nematic phase upon 90° rotation of the sample in the field is explained in terms of a rearrangement of the silica network. Below the gelation threshold, this field-induced realignment is complete, that is, no angular dependence is observed. At higher silica concentrations, still below 0.1 g/cm<sup>3</sup>, the rearrangement appears to be only partial, and by further increasing the aerosil density, the aligning effect of the magnetic field is suppressed and silica-induced disorder dominates.

Apart from the change in the structure and the reduction of order, silica particles have, as already mentioned, dynamic effects leading at macroscopic level to glassy behavior. The dynamic aspects of 4-*n*-heptyl-4'-cyanobiphenyl (7CB) liquid crystal containing a type 300 hydrophilic aerosil dispersion were recently studied by Hourri et al.<sup>18</sup> using dielectric relaxation spectroscopy. The time scale for the reorientation of the molecular long axis was found to be essentially bulklike, with a relaxation time  $\tau \approx 10^{-8}$  s for aerosil densities up to 0.226 g/cm<sup>3</sup>. The Hourri et al. study extends and confirms the results of a previous work of Abd-El-Messieh et al.<sup>19</sup> in which alkylanilines were used as the liquid crystal component. A glasslike relaxation behavior was recently found by Aliev and Sinha<sup>20</sup> in a dispersion of a type 200 hydrophilic aerosil in 5CB liquid crystal, using dynamic light scattering. These works are particularly interesting for us, even if they use a different aerosil type (hydrophilic vs hydrophobic), because they represent, to our knowledge, the only studies dealing with molecular

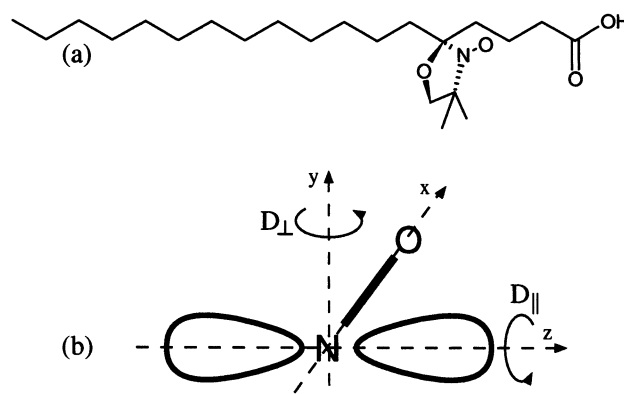


**Figure 1.** Structure (a) of the 5DS spin probe and (b) molecular frame and principal components  $D_{\perp}$  and  $D_{\parallel}$  of the rotational diffusion tensor of 5DS in the liquid crystal for the reorientation of the molecular long axis or for the rotation around it, respectively.

rotational dynamics in filled nematics, even if with a spatial scale larger than our strictly molecular one.

Molecular studies seem to be particularly timely to examine the nature of the glassy behavior found with scattering and turbidity techniques, which have shown relaxation times on scales of milliseconds and even longer.<sup>21</sup> In this paper, we shall concentrate on a molecular level study of a dispersion of the type R812 hydrophobic aerosil in the 8CB liquid crystal by means of the spin probe technique, which consists of adding to the system a stable paramagnetic probe (typically a suitable nitroxide) at a very low concentration (usually  $\sim 10^{-4}$  M) and recording its electron spin resonance (ESR) spectrum in different conditions.<sup>22–24</sup> The method has the specific feature of being local on a molecular scale and being indifferent to turbidity. The analysis of the spectra will provide information on the different local probe environments. In particular, we are interested in changes in the spin probe order and dynamics as the silica concentration and the temperature are varied. We also intend to examine whether the glassy behavior already mentioned is a true one arising even at molecular level.

## 2. Experimental Section

The liquid crystal 8CB was obtained from Merck KGaA (Darmstadt, Germany). This compound exhibits, on heating, the nominal phase sequence crystal–SmA (294.7 K), SmA–N (306.7 K), N–I (313.7 K), as reported by the manufacturer, and was used without further purification. The nitroxide spin probe was the 2-(3-carboxypropyl)-4,4-dimethyl-2-tridecyl-3-oxazolidinyloxy (5-DOXYL-stearic acid, hereafter referred to as 5DS) free radical. It was obtained from Aldrich and was chosen because it is well-ordered by the liquid crystal host and has been used in a number of studies.<sup>25,26</sup> The 5DS structural formula is shown in Figure 1 together with the chosen molecular axis system, which is based on the standard system of coordinates for the N–O paramagnetic moiety with the *x* axis along the N–O bond and the *z* axis parallel to the nitrogen  $p_z$  orbital containing the unpaired electron density. In this way, the *z* axis of the molecular frame is approximately parallel to the long axis of the probe, at least in the fully stretched, all trans conformation. For this compound, dissolved in the 8CB liquid crystal, the principal *g* factors and hyperfine splitting tensor components used were  $g_{xx} = 2.0089$ ,  $g_{yy} = 2.0058$ , and  $g_{zz} = 2.0021$ , corresponding to the standard literature values,<sup>25</sup> and  $A_{xx} = A_{yy} = 5.92$  G and  $A_{zz} = 31.42$  G (1 G =  $10^{-4}$  T), which correspond to the literature values<sup>25</sup> corrected for the polarity of the environment so as to recover the scalar hyperfine

constant  $a = 14.414$  G that we observed experimentally. In a preliminary series of measurements, the spin probe 4-oxo-2,2,6,6-tetramethyl-1-piperidinyloxy (4-Oxo-TEMPO) free radical was also used, but its negligible alignment did not recommend it for this type of experiments.

The aerosil (pyrogenic silicon dioxide) employed was the Degussa<sup>2</sup> type R812, a modified hydrophobic aerosil in which a large part of the surface SiOH (silanols) is protected by methyl groups with a density of only 0.29 free OH groups/nm<sup>2</sup>.<sup>27</sup> The primary particles have a size on the order of 7 nm and do not exist in isolation but form aggregates and agglomerates with a very large surface area (typically  $260 \pm 30$  m<sup>2</sup>/g), which is almost entirely external and is not derived from any porosity.<sup>28</sup>

The 8CB-aerosil samples were prepared according to the solvent method described by Iannacchione et al.<sup>10</sup> and Haga et al.<sup>29</sup> with some modifications. The aerosil was dried under vacuum at  $\sim 150$  °C for 24 h,<sup>30</sup> weighted in dry atmosphere, and mixed with HPLC grade acetone to obtain a  $\sim 0.01$  g/cm<sup>3</sup> suspension, which is not stable and forms a visible sediment in a few minutes. To avoid this problem and achieve a better suspension, the aerosil stock solution was treated for 20 min at maximum power with an ultrasonic homogenizer (Fisher-Artek-Dynatech Sonic Dismembrator, model 150), which operates by immersion via a titanium transducer tip. In this way, we were able to obtain a stable aerosil dispersion, which did not form any sediment over a period of months. A 5DS/8CB stock solution in HPLC-grade acetone was prepared, typically at an 8CB concentration of 0.1–0.3 g/cm<sup>3</sup> with a spin probe concentration of  $3 \times 10^{-4}$  g 5DS/g 8CB. Individual samples were prepared by mixing in acetone the required volume of the 5DS/8CB stock solution and of the aerosil stock solution to a final [8CB] typically of 0.02 g/cm<sup>3</sup>. Because of the very good dispersion of the aerosil stock solution, the samples were then only mechanically mixed but not further sonicated, thus avoiding potential drawbacks due to the interaction of the material of the tip with the spin probe. After stripping of the solvent in an anhydrous nitrogen stream at a temperature of  $\sim 333$  K, the samples were placed in a vacuum system at  $10^{-2}$  mbar (1 mbar =  $10^2$  Pa) and pumped on for 6 h at  $\sim 323$  K. The final samples appeared uniform upon visual inspection, showing no agglomeration when checked with a microscope.

In addition to these, a series of samples was prepared by a mechanical mixing method without using any solvent. Here, the aerosil was directly added to a mixture of 5DS/8CB with a spin probe concentration of  $3 \times 10^{-4}$  g 5DS/g 8CB. This was done to allow a comparison of the effects of the preparation technique and of the “aging” of the samples. Detailed results of this study will be presented in a separate work. Regardless of the preparation method, in all of the samples stored in the ESR tube at room temperature, we noticed a sedimentation of the aerosil that, however, in the case of the solvent method preparation extended over a period of a few weeks. Sedimented samples exhibit a lower probe-order parameter, which returns to the original value after remixing. To avoid this problem, all data were obtained using fresh samples. An on-scale schematic representation of the aerosil dispersion in the liquid crystal is shown in Figure 2.

ESR spectra were recorded with a Bruker ESP300E spectrometer equipped with an ER 041XG microwave X-band (9.5 GHz) Gunn diode bridge and a rectangular ER 4102ST cavity. The sample was contained in a Suprasil quartz tube of 2.4 mm i.d. (Wilmad), thermostated with a nitrogen flux through a variable temperature unit Bruker B-VT 2000. The sample temperature was monitored with a calibrated type T thermo-

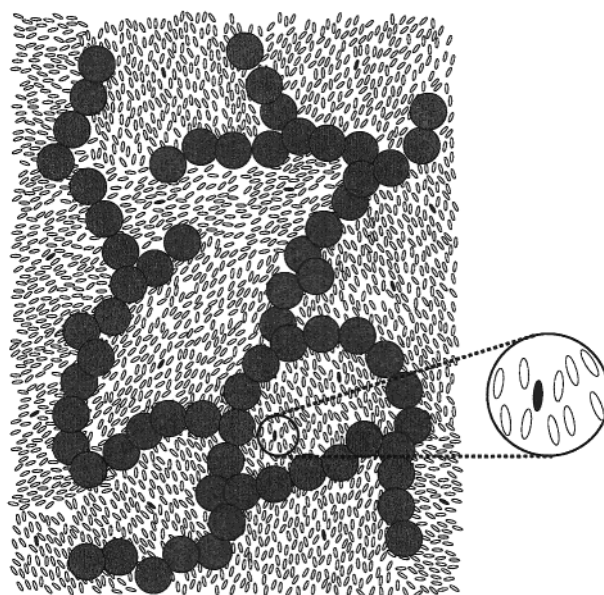


**Figure 2.** On scale schematic representation of the aerosil dispersion showing probe molecules (black particles, see inset) dissolved in the liquid crystal local ordered domains (white particles) and the silica network (gray circles).

couple (Comark Ltd.) inserted into the sample tube and immersed by 10 mm into the upper part of the sample. Tube position and amount of sample (typically 45 mm from tube's bottom) were carefully tested and optimized so as to keep the temperature probe outside the cavity area thus avoiding any possible interference. The accuracy on the temperature control and measurements was better than 0.05 K.

### 3. Theory

The probe is assumed to reorient in a local ordered domain with local director orientation,  $\Omega_{\text{dir}}$ , with respect to the laboratory frame determined by the interaction with the neighboring silica twigs. A sketch of the aerosil showing the local ordered domains and the probe is shown in Figure 2. Reorientation in this local domain can be fast or slow. The resulting ESR spectrum,  $I_p$ , at frequency  $\omega$  is given by the superposition of the ones of the individual domains (the so-called poly-liquid crystalline spectrum<sup>31</sup> or microscopic order–macroscopic disorder (MOMD)<sup>32</sup> model):

$$I_p(\omega - \omega_0) = \int d\Omega_{\text{dir}} P(\Omega_{\text{dir}}) I(\omega - \omega_0; \Omega_{\text{dir}}) \quad (1)$$

where  $\omega_0 = g_0 \beta_e B_0 / \hbar$  and  $P(\Omega_{\text{dir}})$  represents the unknown local director distribution. For practical purpose, we can assume a uniaxial director distribution  $P(\beta_{\text{dir}})$  so that

$$P(\Omega_{\text{dir}}) \equiv P(\beta_{\text{dir}}) \propto \exp[aP_2(\cos \beta_{\text{dir}})] \quad (2)$$

where  $\beta_{\text{dir}}$  is the angle between the local domain director and the magnetic field,  $P_2$  is a second rank Legendre polynomial, and  $a$  is a positive constant. This approach clearly comprises the limiting cases of a completely random domain distribution,  $P(\beta_{\text{dir}}) = 1/\pi$ , and of a monodomain aligned parallel to the magnetic field where  $P(\beta_{\text{dir}}) = \delta(\beta_{\text{dir}})$ . It is well-known that spectra for the two limiting cases are clearly different, indicating that the ESR technique is suitable for this kind of investigation of the system structure. In general, the order of the domains can be characterized by a second-rank orientational order parameter,  $\langle P_2 \rangle_{\text{dir}}$ , for the local director:



$$\langle P_2 \rangle_{\text{dir}} = \frac{\int P_2(\cos \beta_{\text{dir}}) \exp[aP_2(\cos \beta_{\text{dir}})] \sin \beta_{\text{dir}} d\beta_{\text{dir}}}{\int \exp[aP_2(\cos \beta_{\text{dir}})] \sin \beta_{\text{dir}} d\beta_{\text{dir}}} \quad (3)$$

The monodomain spectrum,  $I(\omega - \omega_0, \beta_{\text{dir}})$  at frequency  $\omega$  is obtained using the standard stochastic Liouville equation (SLE) approach of Freed and collaborators,<sup>22–24</sup> which we just summarize very concisely and which predicts that

$$I(\omega - \omega_0; \beta_{\text{dir}}) = \frac{1}{\pi} \langle \langle v | [(\hat{\Gamma} - i\mathcal{L}) + i(\omega - \omega_0)I]^{-1} | v \rangle \rangle \quad (4)$$

where  $\mathcal{L}$  is the Liouville superoperator obtained from the orientation-dependent spin Hamiltonian,  $\Gamma$  is the stochastic evolution operator describing the changes in the orientation  $\Omega$  of the probe in its local domain,  $|v\rangle$  is a vector containing spin transition moments averaged over the equilibrium ensemble, and  $I$  is the identity. The matrix elements of  $\bar{\Gamma}$ , assuming the probe reorientation to be diffusional, are<sup>22–24</sup>

$$\langle \langle \sigma_1 | \hat{\Gamma} | \sigma_2 \rangle \rangle = \delta_{L_1, L_2} \delta_{M_1, M_2} \delta_{K_1, K_2} \delta_{p_1^s, p_2^s} \delta_{q_1^s, q_2^s} \delta_{p_1^I, p_2^I} \delta_{q_1^I, q_2^I} \{ D_{\perp} L_1 (L_1 + 1) + (D_{\parallel} - D_{\perp}) K_1^2 \} \quad (5)$$

where

$$|\sigma_n\rangle = \left( \frac{2L+1}{8\pi^2} \right)^{1/2} D_{M,K}^L(\Omega) |p_n^S, q_n^S; p_n^I, q_n^I\rangle \quad (6)$$

is the spin-orientational space basis set and  $D_{\parallel}$  and  $D_{\perp}$  are the principal components of the rotational diffusion tensor of the probe for rotations around its long or short axis, respectively. In practice, the basis set is obtained from the direct product of the electron spin,  $S$ , with the nuclear spin,  $I$ , eigenfunctions

$$|p^S, q^S; p^I, q^I\rangle = (|S, m_S\rangle \langle S, m'_S|) (|I, m_I\rangle \langle I, m'_I|) \quad (7)$$

while  $D_{M,K}^L$  are the orientational Wigner rotation matrixes with  $L$ ,  $M$ , and  $K$  integers,  $L \geq 0$  and  $|M|$  and  $|K| \leq L$ , forming the basis set for the orientations. The reorientational motion of the probe is assumed to take place in the local mean field ordering potential

$$U(\Omega) = -kT \{ \lambda_{20} D_{00}^2(\Omega) \} \quad (8)$$

which is also employed, when needed, to calculate local orientational order parameters

$$\langle P_L \rangle \equiv \langle D_{0,0}^L \rangle = \frac{\int D_{0,0}^L(\Omega) \exp(-U(\Omega)/(kT)) d\Omega}{\int \exp(-U(\Omega)/(kT)) d\Omega} \quad (9)$$

where  $\Omega$  gives the probe orientation with respect to the local director and  $\lambda_{20}$  is the strength of the potential.

#### 4. Results and Discussion

Four 5DS/8CB samples were studied, either without aerosil or with 1, 3, and 10 wt % R812 (1 wt % R812  $\approx$  0.01 g/cm<sup>3</sup> because 8CB density  $\approx$  0.99 g/cm<sup>3</sup>). For each one, ESR spectra were recorded at 36 different temperatures on heating. Before a typical run, each sample, placed in the cavity under the action of the magnetic field, was subject to the same programmed temperature cycle taking it from room temperature (293–295 K) to 333.2 K (isotropic phase) and then cooling it down slowly to 293.2 K at an average rate of  $\sim$ 2 K/min, which was reduced

to  $\sim$ 0.2 K/min across the phase transitions. At all of the aerosil concentrations studied, this procedure (“field cooling”, FC) was able to anneal the liquid crystal to a monodomain sample. To produce a poly-liquid crystalline distribution of domains, the sample tube, kept outside the magnet, was heated to the isotropic phase and then quickly cooled to  $\sim$ 288 K (8CB crystal phase) to freeze the distribution of domains (“zero-field cooling”, ZFC).<sup>21</sup> At this point, the sample was introduced in the cavity at a temperature lower than that corresponding to the SmA–N transition, and thus, the magnetic field was no longer able to reorient the domains.

ESR spectra were analyzed using a software package that combines an implementation of a modified Gauss–Newton–Marquardt nonlinear least-squares fitting<sup>33</sup> developed in our group<sup>34</sup> with the slow tumbling theory FORTRAN codes for the simulation of the ESR line shapes developed by Freed and collaborators.<sup>22–24</sup> Typical experimental spectra and fit are shown in Figure 3 for the different samples in the SmA, N, and I phase. An example of a poly-liquid crystalline (poly-LC) spectrum in the smectic phase is shown for comparison (Figure 3a).

We also registered and analyzed a few ESR spectra within the nematic and smectic phase on cooling, after the measurements done on heating. In all of the cases, the results did not show a significant difference between a heating and a cooling run.

The order parameter,  $\langle P_2 \rangle_{\text{dir}}$ , of the local director defined with respect to the magnetic field frame and recovered from the analyses of FC samples was always very close to unity ( $>0.99$ ), as expected for a monodomain. As far as the orientational order parameter,  $\langle P_2 \rangle$ , of the spin probe is concerned, we show in Figure 4a its temperature dependence in the monodomain sample at various aerosil concentrations. We notice that our  $\langle P_2 \rangle$  values for the pure (“no aerosil”) system are smaller than those calculated from the NMR quadrupole splitting data of bulk 8CB deuterated on the first carbon position along the hydrocarbon chain (C1) obtained by Jin and Finotello<sup>9</sup> (see Table 1). This difference can be explained by considering the flexibility of the spin probe aliphatic chain in the region where the nitroxide group is located (C5),<sup>26,32</sup> as well as the reduced ordering along the hydrocarbon chain of 8CB. Indeed, Boden et al.<sup>35</sup> studied, in an earlier work, the dependence of the NMR quadrupole splitting of bulk 8CB deuterated on different positions along the hydrocarbon chain. Their data for bulk 8CB deuterated on the first carbon are in good agreement with the results of Jin and Finotello,<sup>9</sup> but they also found smaller quadrupole splitting values for 8CB deuterated on the fifth carbon (C5). Interestingly, the  $\langle P_2 \rangle$  values calculated from these last data are in good agreement with our results (Table 1, last two columns) thus confirming the assumption that the spin probe is, in fact, experiencing a reduced local ordering. A discussion of the dependence of the local ordering of the nitroxide group on its position along the stearic aliphatic chain goes beyond the scope of this work. A detailed investigation along these lines can be found in several works, for example, by Meirovitch, Broido, and Freed<sup>32,36–38</sup> and in references therein.

Going back to Figure 4, we see that, as the aerosil concentration increases, the position of both the SmA–N and the N–I transition is essentially unaffected whereas the N–I transition becomes weaker with, however, a discontinuity of the order parameter remaining in any case visible. The SmA–N transition is also still appreciable even at 10 wt % R812, but, according to Marinelli and Mercuri,<sup>39</sup> the variation of the orientational order parameter at this transition is relatively small. The decrease

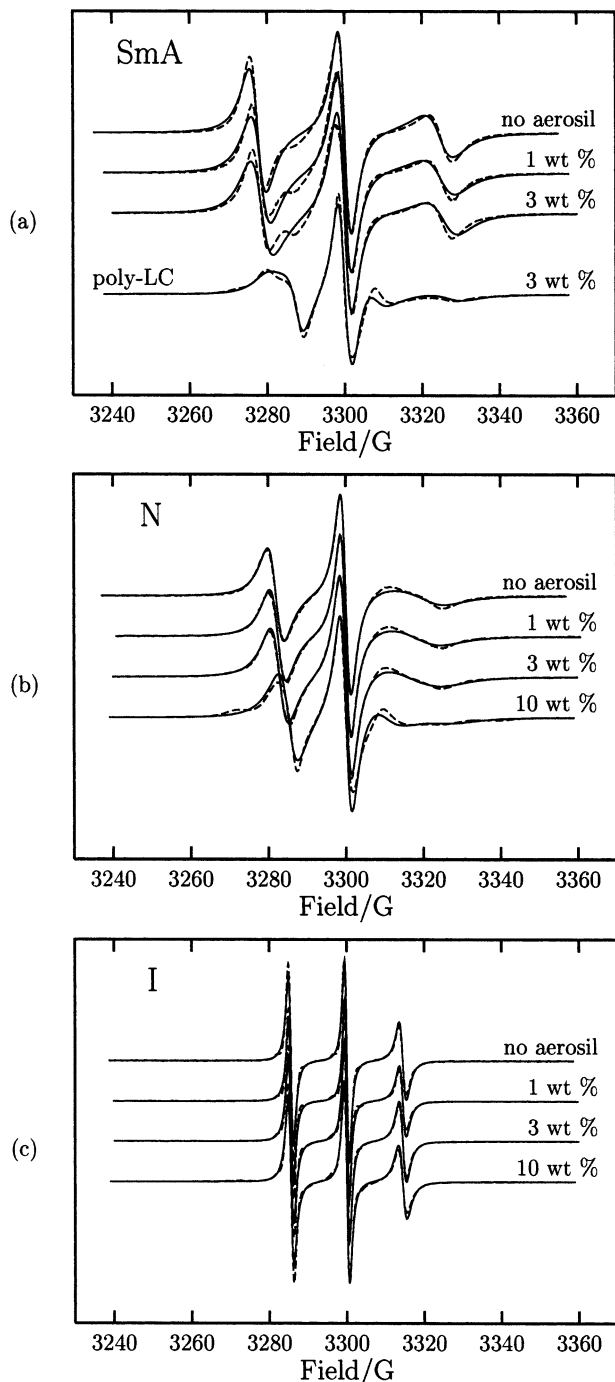


**Figure 3.** Typical experimental spectra (dashed lines) and fit (solid lines) for the monodomain samples in the (a) smectic A ( $T = 295.2$  K), (b) nematic ( $T = 310.2$  K), and (c) isotropic phase ( $T = 343.2$  K) at the various silica concentrations studied. A poly-liquid crystalline (poly-LC) spectrum of the 3 wt % sample in the smectic phase, obtained as described in the text, is shown for comparison in panel a.

of the orientational order parameter with increasing aerosil concentration appears to be roughly linear in the range studied. This result is thus different from that obtained by Jin and Finotello<sup>9</sup> for a type 300 hydrophilic aerosil dispersion in 8CB, where they found that the order parameter of the bulk liquid crystal is almost independent of the aerosil concentration up to  $\sim 10$  wt %. To study the variations in the temperature dependence of  $\langle P_2 \rangle$  induced by the addition of the aerosil, data for the N region, shown in Figure 4b, were fitted to different empirical equations commonly used by several authors.<sup>39,40</sup> Possibly because of the limited number of experimental points

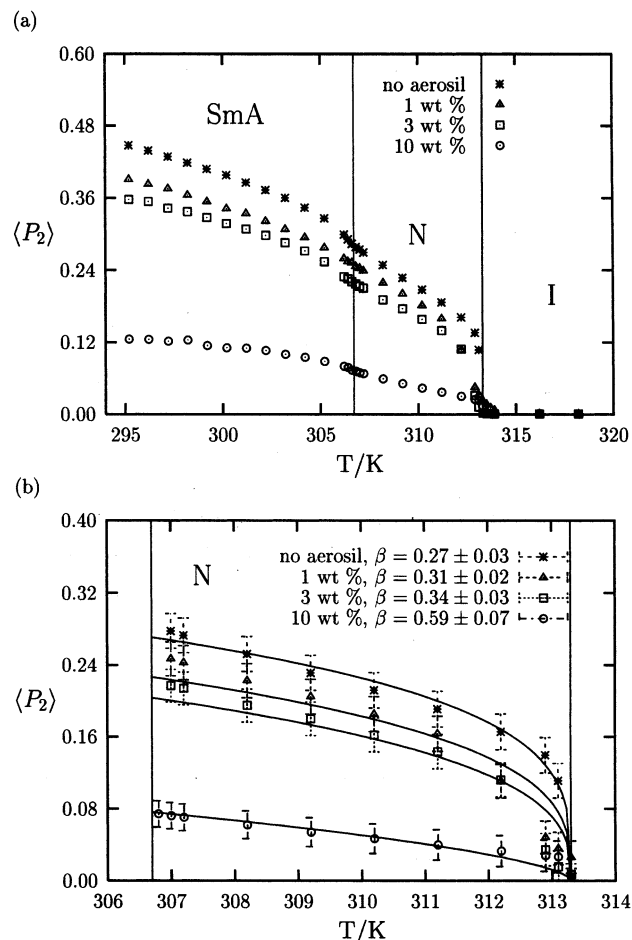


**Figure 4.** Temperature dependence (a) of the orientational order parameter  $\langle P_2 \rangle$  of the spin probe at various aerosil concentrations and (b) detail of the nematic region shown in panel a. The solid lines represent a fit to a Haller-type equation,  $\langle P_2 \rangle = \alpha(1 - T/T_c)^\beta$ , with  $\alpha = 0.76$  and  $T_c = 313.3$  K (see text for details). Best fit values for  $\beta$  are also shown.

**TABLE 1:  $\langle P_2 \rangle$  Values Calculated from NMR Quadrupole Splitting Data of 8CB Deuterated on the First (C1) or on the Fifth (C5) Position of the Aliphatic Chain Compared to the Values Obtained in This Work for the 5DS Spin Probe**

| $T$ , K | C1 <sup>9</sup> | C1 <sup>35</sup> | C5 <sup>35</sup> | this work |
|---------|-----------------|------------------|------------------|-----------|
| 300.2   | 0.59            | 0.56             | 0.39             | 0.40      |
| 304.2   | 0.53            | 0.50             | 0.33             | 0.34      |
| 308.2   | 0.41            | 0.36             | 0.20             | 0.25      |

available from our measurements in the N phase and, in particular, close to the N–I transition, none of these analyses gave stable and uncorrelated parameters. A better choice to describe the data in our temperature range is represented by the simpler Haller-type equation:<sup>41–46</sup>

$$\langle P_2 \rangle = \alpha(1 - T/T_c)^\beta \quad (10)$$

A Haller fit of this kind to the data of Jin and Finotello<sup>9</sup> assuming  $\alpha = 1$  (i.e.,  $\langle P_2 \rangle = 1$  at limiting low temperature) gave  $\beta = 0.18$ . Here for our flexible probe, we could not assume a priori  $\alpha = 1$ , and thus, we have fitted our data for the silica-free sample allowing  $\alpha$ ,  $T_c$ , and  $\beta$  as free parameters. The fit showed less correlation than before but yielded a poor estimation of the  $T_c$  value. Therefore, we fixed  $T_c$  at the value of 313.3 K, which is the temperature at which the  $\langle P_2 \rangle$  drops to zero according to our ESR measurements. This gave  $\alpha = 0.76$ , which we have then kept fixed as a probe related parameter for all the

other cases studied, and  $\beta = 0.27$ . The difference between this  $\beta$  value and that ( $\beta = 0.18$ ) obtained from the data of Jin and Finotello<sup>9</sup> could once more be attributed to the difference between using an intrinsic or extrinsic probe (different positions monitored along the 8CB chain). The fitted curves for all of the cases studied are reported in Figure 4b (solid lines), together with best fit values for  $\beta$ . As the aerosil concentration increases, we found that the variation of  $\beta$  appears to be approximately linear.

Because the analysis relies on the values assumed for the magnetic parameters of the probe and, in particular, on the value assumed for the hyperfine constant  $a$ , which is, to a scaling factor, polarity-dependent, to estimate the uncertainty on  $\beta$ , 10 values of  $a$  were sampled from a Gaussian distribution centered at the experimental value of 14.414 G and with a standard deviation of 1%. For each value of  $a$ , the entire series of fits of the ESR spectra was repeated, yielding a distribution of  $\langle P_2 \rangle$  values indicated by the error bars in Figure 4b. This distribution was then used to repeat the Haller fit to obtain a distribution of  $\beta$  values of which the statistics is indicated in the legend of Figure 4b at a confidence interval of 95%.

The temperature dependence of the tumbling diffusion coefficient,  $D_{\perp}$ , for the nitroxide at various aerosil concentrations is shown in Figure 5a. The values recovered are consistent with those obtained for stearic acid spin probes in similar liquid crystal systems.<sup>36,38</sup> It is very interesting to observe that the rotational dynamics is only slightly affected by the presence of the aerosil even at a concentration of 10 wt %, at which the macroscopic viscosity of the sample is quite high (the sample does not flow), and at the highest temperature studied. For the I phase, we found that  $D_{\perp}$  obeys a simple Arrhenius-type equation:  $D_{\perp} = D_{\perp}^0 \exp(-E/RT)$  (solid lines). Best fit values for the activation energy  $E$  are shown in Figure 5a and correspond to a preexponential factor  $D_{\perp}^0$  of  $(2 \pm 1) \times 10^{15} \text{ s}^{-1}$ . In the N phase (Figure 5b), for a silica concentration up to 3 wt %, the tumbling diffusion coefficient still exhibits an Arrhenius-like behavior (solid lines) except in the vicinity of  $T_c$ , with values for  $E$  (see figure), which are, as expected, larger than those observed in the I phase but essentially concentration-independent. For both the N and the I phase, best fit values for  $E$  are in agreement with those found in a dielectric relaxation work by Schönhalz et al.<sup>47</sup> on unaligned 8CB and in references therein. A deviation from an Arrhenius behavior, already present in the 3 wt % aerosil data, of which the fit was slightly poorer than those of the pure and of the 1 wt % systems, is clearly visible in the 10 wt % data (lower solid line). These data were found instead to obey the Vogel–Fulcher–Tammann (VFT) equation<sup>48–50</sup>

$$D_{\perp} = D_{\perp}^0 \exp[-B/(T - T_0)] \quad (11)$$

where  $B$  is a temperature corresponding to an activation energy  $RB$  and  $T_0$  is the Vogel–Fulcher–Tammann temperature of the system. This behavior is typical of several glass-former materials, thus indicating the presence of a different viscosity regime at increasing aerosil concentrations (dashed line). Best fit values for the 10 wt % data are shown in Figure 5b, with  $D_{\perp}^0 = 1 \times 10^{18} \text{ s}^{-1}$ . We notice that the value of 106 K found for  $T_0$  in this silica-filled 8CB sample is, as expected, smaller than the glass transition temperature,  $T_g = 207 \text{ K}$ , found for similar cyanobiphenyl liquid crystals.<sup>51</sup>

From these results, it would seem that the 10 wt % R812 sample is in a glassy state also at the molecular level, while the 3 wt % sample is borderline. To test this aspect, we considered

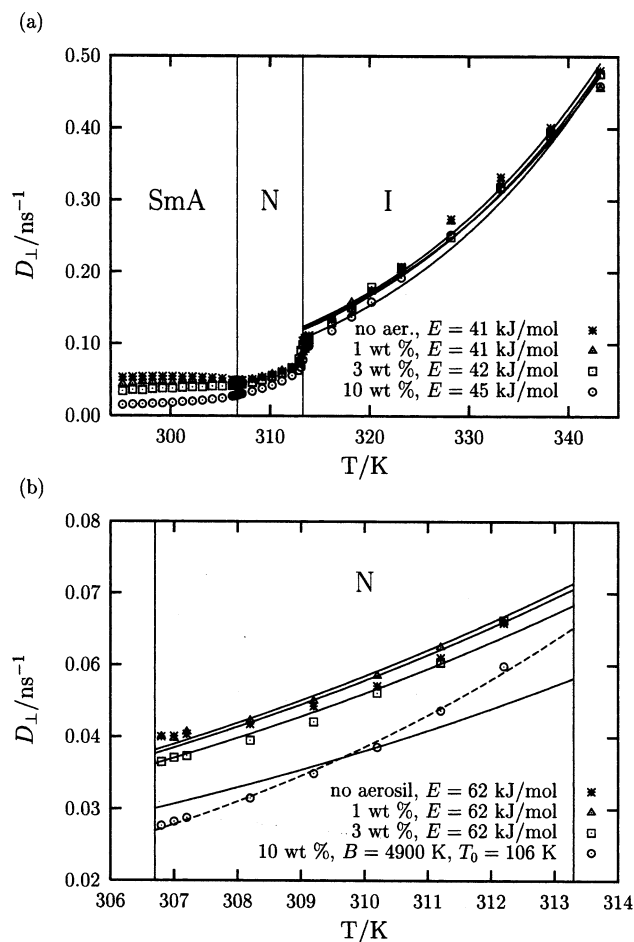


**Figure 5.** Temperature dependence (a) of the tumbling diffusion coefficient  $D_{\perp}$  of the spin probe at various aerosil concentrations. Data in the isotropic (I) phase obey a simple Arrhenius-type equation,  $D_{\perp} = D_{\perp}^0 \exp(-E/RT)$  (solid lines). Best fit values for the activation energy  $E$  are also shown;  $D_{\perp}^0 = (2 \pm 1) \times 10^{15} \text{ s}^{-1}$ . Panel b shows detail of the nematic region shown in panel a. Experimental data points in the vicinity of  $T_c$  (above  $T = 312.2 \text{ K}$ ) have been removed. Solid lines represent the fit to the Arrhenius equation; dashed lines represent the fit to the Vogel–Fulcher–Tammann equation (see text for details).

that glassy systems at the same temperature can have a different behavior according to their history and preparation. We have thus examined a 3 wt % sample cooled outside the spectrometer (ZFC) at a temperature ( $T = 295.2 \text{ K}$ ) inside the SmA phase for which the magnetic field cannot realign it. This sample is certainly glassy at macroscopic level (from its scattering and no flow appearance), and its ESR spectrum, as shown in Figure 3a (“poly-LC”), is of powder type. The analysis of this spectrum yielded a quasi-random distribution of local domains with a  $\langle P_2 \rangle_{\text{dir}}$  of 0.19, a local orientational order parameter  $\langle P_2 \rangle$  of 0.33, and a tumbling diffusion coefficient of  $0.02 \text{ ns}^{-1}$ , values similar to those found for the monodomain sample at the same temperature (see corresponding points in Figures 4a and 5a). This result shows that the local order and dynamics are independent of the overall structure of the sample indicating that the 3 wt % system is macroscopically a glass but appears to be a fluid at the molecular level.

In summary, we have found that the addition of the hydrophobic R812 aerosil, at the concentrations studied, has a strong effect on the ordering of a stearic spin probe dissolved in the 8CB liquid crystal. The rotational dynamics of the system is more complex. Examining the individual values of the diffusion coefficient at a certain temperature, we found that,



increasing the aerosil concentration, they do not show the strong differences that one might have expected on the basis of the large changes of the macroscopic viscosity of the system ranging, for example, in the I phase from that of a fluid for the pure system to that of a gel at 10 wt % aerosil. This apparent independence of the rotational dynamics on the aerosil concentration was also observed by Hourri et al.<sup>18</sup> who found, using dielectric relaxation spectroscopy, that the rotational relaxation time for the 7CB plus type 300 hydrophilic aerosil samples almost coincided with that of the pure system for aerosil densities up to 0.226 g/cm<sup>3</sup> (~23 wt %). They discussed their results assuming that the dispersion could be considered as a collection of nematic domains (see Figure 2) in which the liquid crystal behavior is essentially bulklike. This discussion would seem to be appropriate also for our system, if we consider, at least qualitatively, the kind of aerosil network that should be present. Assuming that the surface area (~260 m<sup>2</sup>/g for the R812 aerosil<sup>28</sup>) is due only to the external surface of the primary particles, it is possible to estimate a number density of  $\sim 1.7 \times 10^{18}$  particles/g, which in practice means having fairly large "pools" of liquid crystal among the aerosil network, where it seems reasonable to observe a bulklike behavior.

However, examining not just the individual values of the diffusion coefficient but also their temperature dependence in the N phase, we have the experimental indication that the system, above a certain level of quenched disorder, exhibits a change from an Arrhenius-like to a Vogel–Fulcher–Tammann behavior. This result indicates that also a low aerosil concentration, as is the 10 wt %, is able to modify the behavior at the molecular level from that of a fluid to that of a fragile glass.

## 5. Conclusions

The picture emerging from our studies, in conjunction with the optical and simulation ones from literature,<sup>3,4,16,21</sup> suggests a very rich behavior of the aerosil-filled nematics corresponding to that of a macroscopically viscous fluid with a local high mobility, similar to that of the unperturbed nematic. The slowing of the dynamics employed in the filled nematic ("memory") effect appears then to be essentially macroscopic. The permanence of local fluidity can help to rationalize the fast switching response time of the system. When the aerosil concentration increases, the temperature dependence of the dynamics becomes glasslike even at the molecular level. This change of behavior takes place at a silica concentration above 3 wt % and is clearly visible at 10 wt %.

**Acknowledgment.** We thank MURST (PRIN "Cristalli Liquidi"), CNR PF MSTA II, and the University of Bologna for support. We also thank Prof. T. Bellini and Dr. F. Mantegazza for the aerosil samples, Dr. C. Cassani and Dr. L. Vitale for help with the sample preparation, Prof. A. Alberti and Dr. D. Macciantelli for their ESR instrumentation used in an extra series of measurements, and Dr. P. Pasini for stimulating discussions.

## References and Notes

- (1) Chandrasekhar, S. *Liquid Crystals*, 2nd ed.; Cambridge University Press: Cambridge, U.K., 1977.
- (2) *Aerosils*; Degussa Corp., Silica Division: Frankfurt, Germany, 2000.
- (3) Bellini, T.; Buscaglia, M.; Chiccoli, C.; Mantegazza, F.; Pasini, P.; Zannoni, C. *Phys. Rev. Lett.* **2000**, *85*, 1008.
- (4) Kreuzer, M.; Eidschink, R. In *Liquid Crystals in Complex Geometries*; Crawford, G. P., Zumer, S., Eds.; Taylor & Francis: London, 1996; Chapter 15, p 307.
- (5) Imry, Y.; Ma, S. K. *Phys. Rev. Lett.* **1975**, *35*, 1399.
- (6) Kreuzer, M.; Tschudi, T.; Eidschink, R. *Mol. Cryst. Liq. Cryst.* **1992**, *223*, 219.
- (7) Eidschink, R.; de Jeu, W. H. *Electron. Lett.* **1991**, *27*, 1195.
- (8) Kreuzer, M.; Tschudi, T.; de Jeu, W. H.; Eidschink, R. *Appl. Phys. Lett.* **1993**, *62*, 1712.
- (9) Jin, T.; Finotello, D. *Phys. Rev. Lett.* **2001**, *86*, 818.
- (10) Iannacchione, G. S.; Garland, C. W.; Mang, J. T.; Rieker, T. P. *Phys. Rev. E* **1998**, *58*, 5966.
- (11) Mercuri, F.; Ghosh, A. K.; Marinelli, M. *Phys. Rev. E* **1999**, *60*, 6309.
- (12) Marinelli, M.; Ghosh, A. K.; Mercuri, F. *Phys. Rev. E* **2001**, *63*, 61713.
- (13) Zhou, B.; Iannacchione, G. S.; Garland, C. W.; Bellini, T. *Phys. Rev. E* **1997**, *55*, 2962.
- (14) Wu, L.; Zhou, B.; Garland, C. W.; Bellini, T.; Schaefer, D. W. *Phys. Rev. E* **1995**, *51*, 2157.
- (15) Radzihovsky, L.; Toner, J. *Phys. Rev. Lett.* **1997**, *79*, 4214.
- (16) Glushchenko, A.; Kresse, H.; Reshetnyak, V.; Reznikov, Y.; Yaroshchuk, O. *Liq. Cryst.* **1997**, *23*, 241.
- (17) Hauser, A.; Kresse, H.; Glushchenko, A.; Yaroshchuk, O. *Liq. Cryst.* **1999**, *26*, 1603.
- (18) Hourri, A.; Bose, T. K.; Thoen, J. *Phys. Rev. E* **2001**, *63*, 51702.
- (19) Abd-El-Messieh, S. L.; Werner, J.; Schmalfuss, H.; Weissflog, W.; Kresse, H. *Liq. Cryst.* **1999**, *26*, 535.
- (20) Aliev, F.; Sinha, G. *Mol. Cryst. Liq. Cryst.* **2001**, *364*, 435.
- (21) Bellini, T.; Buscaglia, M.; Chiccoli, C.; Mantegazza, F.; Pasini, P.; Zannoni, C. *Phys. Rev. Lett.* **2002**, *88*, 245506.
- (22) Freed, J. H. In *Electron Spin Relaxation in Liquids*; Muus, L. T., Atkins, P. W., Eds.; Plenum Press: New York, 1972; Chapter 14, p 387.
- (23) Freed, J. H. In *Spin Labeling. Theory and Applications*; Berliner, L. J., Ed.; Academic Press: New York, 1976; Chapter 3, p 53.
- (24) Schneider, D. J.; Freed, J. H. In *Biological Magnetic Resonance. Spin Labeling*; Berliner, L. J., Reuben, J., Eds.; Plenum Press: New York, 1989; Vol. 8, Chapter 1.
- (25) *Spin Labeling. Theory and Applications*; Berliner, L. J., Ed.; Academic Press: New York, 1976.
- (26) Zhang, J.; Lux, Z.; Zimmermann, H.; Goldfarb, D. *J. Phys. Chem. B* **2000**, *104*, 279.
- (27) Chuiko, A. A.; Gorlov, Y. I. *Chemistry of a silica surface*; Naukova Dumka: Kyiv, Ukraine, 1992.
- (28) Michael, G.; Ferch, H. *Basic Characteristics of AEROSIL*; Technical Bulletin Pigments No. 11; Degussa: Frankfurt, Germany, 1993.
- (29) Haga, H.; Garland, C. W. *Phys. Rev. E* **1997**, *56*, 3044.
- (30) Perrin, D. D.; Armarego, W. L. F.; Perrin, D. R. *Purification of laboratory chemicals*; Pergamon Press: Oxford, U.K. 1988.
- (31) Zannoni, C.; Pedulli, G. F.; Masotti, L.; Spisni, A. *J. Magn. Reson.* **1981**, *43*, 141.
- (32) Meirovitch, E.; Nayeem, A.; Freed, J. H. *J. Phys. Chem.* **1984**, *88*, 3454.
- (33) Bevington, P. R. *Data Reduction and Error Analysis for the Physical Sciences*; McGraw-Hill: New York, 1969.
- (34) Arcioni, A.; Tarroni, R.; Zannoni, C. *J. Chem. Soc., Faraday Trans.* **1993**, *89*, 2815.
- (35) Boden, N.; Clark, L. D.; Bushby, R. J.; Emsley, J. W.; Luckhurst, G. R.; Stockley, C. P. *Mol. Phys.* **1981**, *42*, 565.
- (36) Broido, M. S.; Meirovitch, E. *J. Phys. Chem.* **1983**, *87*, 1635.
- (37) Meirovitch, E.; Freed, J. H. *J. Phys. Chem.* **1984**, *88*, 4995.
- (38) Meirovitch, E.; Broido, M. S. *J. Phys. Chem.* **1984**, *88*, 4316.
- (39) Marinelli, M.; Mercuri, F. *Phys. Rev. E* **2000**, *61*, 1616.
- (40) De Gennes, P. G.; Prost, J. *The Physics of Liquid Crystals*, 2nd ed.; Clarendon: Oxford, U.K., 1993.
- (41) Haller, I. *Prog. Solid State Chem.* **1975**, *10*, 103.
- (42) Bender, M.; Holstein, P.; Geschke, D. *Liq. Cryst.* **2001**, *28*, 1813.
- (43) Canlet, C.; Fung, B. M. *Liq. Cryst.* **2001**, *28*, 1863.
- (44) Sun, H.; Roth, M. D.; Fung, B. M. *Liq. Cryst.* **2001**, *28*, 1469.
- (45) Wu, S. T.; Cox, R. J. *J. Appl. Phys.* **1988**, *64*, 821.
- (46) Leenhouts, F.; de Jeu, W. H.; Dekker, A. J. *J. Phys.* **1979**, *40*, 989.
- (47) Schönhals, A.; Zubowa, H. L.; Fricke, R.; Frunza, S.; Frunza, L.; Moldovan, R. *Cryst. Res. Technol.* **1999**, *34*, 1309.
- (48) Vogel, H. *Phys. Z.* **1921**, *22*, 645.
- (49) Fulcher, G. S. *J. Am. Ceram. Soc.* **1925**, *8*, 339.
- (50) Tammann, V. G.; Hesse, W. Z. *Anorg. Allg. Chem.* **1926**, *156*, 245.
- (51) Schadt, H.; Zeller, H. R. *Phys. Rev. A* **1982**, *26*, 2940.